Plunge testing to evaluate tool materials for friction stir welding of 6061+20wt%Al_2O_3 composite

Michael Santella, Oak Ridge National Laboratory, Oak Ridge, Tennessee, USA

Glenn Grant, Pacific Northwest National Laboratory, Richland, Washington, USA

William Arbegast, South Dakota School of Mines and Technology, Rapid City, South Dakota, USA

Abstract

A simple plunge test was used to evaluate some of the interactions between 6061 + 20 wt% Al_2O_3 plates and flat-faced, cylindrical pin tools of H13 steel, WC bonded with 10 wt% Co, and gas pressure sintered Si_3N_4. The 12.5-mm-diameter pin tools were rotated at 800 rpm under a normal force of 13,344 N and then driven into the plates to a depth of approximately 10 mm. Each test consisted of two segments, a constant-displacement-control plunge to a depth of 1.5 mm followed by a constant-force-control plunge from 1.5 mm to about 10 mm. The forces supported by the pin tools in the constant displacement segments varied with pin tool material. The displacement rates supported by the pin tools in the constant force segment varied with pin tool material. Normal force and spindle torque measurements were used to calculate effective friction coefficients, μ_{eff}, for each pin tool material on the 6061/Al_2O_3. These values were: μ_{eff} = 1.024 for the H13, μ_{eff} = 0.768 for the WC10Co, and μ_{eff} = 0.621 for the Si_3N_4. The variations in behavior for the pin tools were attributed to the effect of μ_{eff} on frictional heating. An accumulation of the 6061/Al_2O_3 was found on the H13 pin tool after testing but not on pin tools of the other two materials.

Introduction

There are a fairly wide variety of techniques that rely on frictional heating to bond metal [1]. The frictional heating results from rubbing two parts together at high surface speeds under pressure. As the temperature at the region of contact rises to the forging range, the pressure across the interface forces the components together resulting in a metallurgical bond. The more common methods of friction welding rely on rotation to produce the high speed rubbing action. To make effective use of this process, at least one of the parts is often axisymmetric in its shape perpendicular to the bond interface. The rotary variants of friction welding are ideal for making joints in rods and tubing, and for bonding parts of axisymmetric shape to ones that are not. These more traditional methods of friction welding can be applied to a very wide variety of alloys, from lead to refractory metals [1], and they are used routinely to make automotive, aerospace, and medical components.

The requirement of having at least one axisymmetric part of modest diameter is a limitation of rotary friction welding which has been overcome by the invention and development of the friction stir welding process [2]. In friction stir welding, frictional heating is accomplished by

use of a rotating, nonconsumable tool that is translated through the joint while the parts being welded remain stationary [2,3]. Plates can be welded together using the friction stir process, and this has catalyzed considerable interest in it. Friction stir welding is already being used commercially to fabricate various aluminum alloy plate components for marine applications [4], and it is being considered for a number of other situations that require welding of aluminum alloy sheet and plate [5,6].

The friction stir weld zone microstructures are similar to those developed during thermomechanical processing [5,7]. Ideally, melting is avoided so the metallurgical issues associated with solidification during welding are also avoided. Because the peak temperatures experienced during friction stir welding are lower than those of fusion welding processes distortion may be reduced and microstructural changes associated with the welding thermal cycle are minimized. Characteristics such as these make friction stir welding an attractive process for welding a variety of high temperature alloys and metal matrix composites. For these alloys, however, the selection of materials for the rotating nonconsumable tooling are crucial to successful deployment.

Properties that are likely to be important for tool materials include strength, fatigue resistance, wear resistance, thermal conductivity, toughness, and chemical stability. High strength relative to base materials is an absolute necessity for tools. However, the relative importance of other properties is not well understood [3].

The work described in this paper represents an attempt to determine whether a relatively simple plunge test can be used to provide useful insights into any of the interactions between base materials and tool materials.

Experimental Details

The base material used for the experiments was 6061 aluminum containing 20 wt% of aluminum oxide particles. The 6061/Al_2O_3 was supplied as an 280-mm-diameter extruded billet (QED Extrusions Developments Inc., San Diego, CA). The billet was sliced perpendicular to its extrusion axis to provide 19-mm-thick circular plates for the experiments. The plate surfaces were turned to a finish of 0.8 μm average deviation from the mean surface with top and bottom surfaces parallel to ± 50 μm.

Three tool materials were evaluated against the 6061/Al_2O_3: H13 tool steel, a cermet of tungsten carbide bonded with 10 wt% Co, WC10Co, and a gas-pressure-sintered silicon nitride (Kyocera SN282). The tool materials were machined into 12.5-mm-diameter cylindrical pins with flat circular faces.

Typical handbook property values for the 6061/Al_2O_3 and the three tool materials are given in Table 1.

Evaluation of the tool materials consisted of vertically plunging the rotating cylindrical pin tools into the 6061/Al_2O_3 plates. The experiments were conducted on a purpose-built friction stir welding machine with servo-hydraulic actuation of force and displacement functions (MTS

Table 1. Typical properties at room temperature

Material	Thermal conductivity W/m-K	Strength MPa	Fracture toughness MPa-√m
6061+20% Al_2O_3	130	359	18
H13 steel	29	2,000	30
WC-10% Co	100	2,100	10
Si_3N_4	35	800	6

Corporation, Eden Prairie, MN). The procedure consisted of an initial plunge to a depth of 1.5 mm using displacement control. The plunge rate in this segment was 0.1 mm/s. The initial plunge was used to seat the tools into the plate surfaces. Thereafter, the tools were plunged an additional 8 mm into the plates using force control. This means that the displacement rates in the second plunge segment were not controlled by machine settings, rather they were determined by material properties and interactions between the tool materials and the 6061/Al_2O_3. In the force-controlled segments, the tools were programmed to rotate at 800 rpm under a normal load of 13,344 N, values that are in the ranges of those frequently used for friction stir welding of Al alloys. The parameters recorded during the plunging tests included actual normal loads, spindle torques, tool displacements, times, tool rotation speeds, and surface temperatures of the plates.

Results

Figure 1 shows plots of the variations of normal force and torque with pin tool displacement into the 6061/Al_2O_3 plates for the three pin tool materials. Vertical lines are placed at 1.5 mm to distinguish between the segments of the seating plunges and the test plunges. In all three cases, the constant-displacement-rate seating segments show initial spikes in normal load as the rotating pin tools were driven into the plates. The normal forces increased throughout this period, but those measured at the end of the seating segments varied with the tool material. These normal forces were 8,362 N for the H13 tool, 10,991 N for the WC10Co tool, and 13,246 N for the Si_3N_4 tool. During the test segments, the normal forces rapidly approached the requested setpoint of 13,334 N, that is indicated by horizontal lines in Fig. 1.. For the H13 pin tool the measured force never actually attained the setpoint value. In contrast, the 13,344 N force was supported during the test by both the WC10Co and the Si_3N_4 tools.

The measured spindle torques showed initial rapid increases followed by slight gradual increases as the tests were run to completion. The pin rotational speed of 800 rpm was maintained during each test.

The normal force and spindle torque measurements were combined to calculate an effective friction coefficient, μ_{eff}, for each data set using the analysis developed by Cheng [8]. The face of the spinning cylindrical pin tool in contact with the 6061/Al_2O_3 plate surface is characterized by the elementary area, $dA = 2\pi r dr$, as shown in Fig. 2. Then the friction force, F_f, acting on the elementary area is given by:

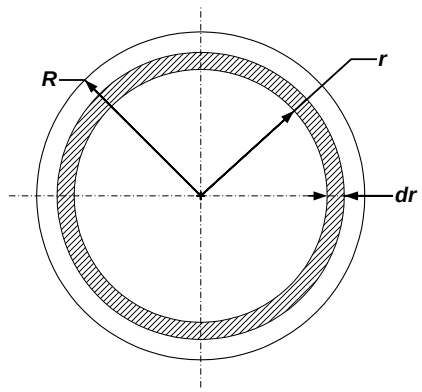

Fig. 2. Schematic of elementary area on pin tool face.

$$dF_f = P\mu_{eff}\, 2\pi r dr$$

where P is the pressure on the pin tool face. Because torque is the product of force and radial distance, the torque, T, on an elementary area of the tool face is:

$$dT = P\mu_{eff}\, 2\pi r^2 dr$$

Assuming that P and μ_{eff} do not vary with position on the tool face, integration of the torque expression and appropriate substitutions lead to the relationship:

$$\mu_{eff} = \frac{3}{2}\frac{T_S}{F_N \times R}$$

where F_N is the normal force on the pin tool, and T_S is the spindle torque. The variations of the effective friction coefficients with displacement are shown in Fig. 3 for the entire data sets including the seating segments. Because the normal force values were erratic and the torque values require finite times to stabilize during seating, the effective friction coefficient values during these segments appear artificially high and variable. The effective friction coefficient values during the force-controlled test segments, for the displacement ranges from 1.5 mm to end of tests, are shown in Fig. 4. In the test segments, beyond the 1.5 mm displacement, the effective friction coefficient values were relatively constant showing only slight increases up to the maximum plunge displacements. The variations of effective friction coefficient values with displacements mirrored those of the torque values as expected. The average effective friction coefficient values during the test segments are also shown in Fig. 4. The average values were μ_{eff} = 1.024 for the H13, μ_{eff} = 0.768 for the WC10Co, and μ_{eff} = 0.621 for the Si_3N_4.

The displacement rates for the tests are shown in Fig. 5. Because plunging was displacement controlled up to a depth of 1.5 mm the initial displacement rates were identical for all three pin tool materials. Beyond 1.5 mm of displacement, the plunging condition was changed to force controlled. In the force-controlled test segments there were clearly significant variations in displacement rates. The average displacement rates in these segments were 0.56 mm/s for H13, 0.18 mm/s for WC10Co, and 0.10 mm/s for Si_3N_4.

The contours of the pins were measured after the tests on a coordinate measuring machine with a 0.7-mm-diameter tungsten carbide stylus. The surface profiles from the centerlines to the outer diameters of the H13 and the Si_3N_4 pin tools are plotted in Fig. 6. The x coordinate values represent radial distance from the centerline. The y coordinate values represent distance from the pin tool faces. The horizontal portions of the traces provide the profiles on the tool faces. In Fig. 6, the profile from the Si_3N_4 pin is offset in the y coordinate direction for clarity. The Si_3N_4 profile clearly shows the chamfer that was machined into the pin. The profile after testing was essentially identical to that measured prior to testing. The H13 pin tool was originally machined to the same shape as the Si_3N_4 tool including the chamfer. However, its profile was significantly

different after testing. Material from the 6061/Al_2O_3 has actually adhered to both the face and the chamfer of the H13 tool. The 6061/Al_2O_3 material accumulated on the H13 tool face in a toroidal ring that extended up to 0.25 mm above the original tool surface. No significant accumulations of 6061/Al_2O_3 were found on either the WC10Co tool or the Si_3N_4 tool after testing.

Optical micrographs taken at the corners of the blind plunge holes are shown in Fig. 7. The bottoms of the holes are on the bottoms of these micrographs. For the H13 tool, Fig. 7a, the profile of the hole is very irregular, and this clearly resulted from fracturing of the 6061/Al_2O_3 caused by its adherence to the tool face. The hole profiles for the WC10Co and Si_3N_4 tools, Fig. 7b and 7c, respectively, were smooth and they provide a direct impression of the shape of these tools including the chamfer details. These micrographs also suggest that any microstructural modifications caused by the plunge tests were localized in the 6061/Al_2O_3 to its interfaces with the various tool materials.

Discussion

The variations of normal force and spindle torque shown in Fig. 1 are similar to those observed during friction welding of aluminum alloys [9]. One important difference between friction stir welding of plates and the plunge test is that steady state conditions may be achieved in welds of sufficient length. In contrast, the geometry and configuration of the plunge test are likely to prevent a true steady state condition from ever being established. For instance, cylindrical pin tools cannot be plunged to infinite depths into plates of finite thicknesses. Consequently, the temperature fields around the pin tools are likely to vary continuously during plunge tests. These effects will depend on the dimensions of the pin tools and the plate thicknesses, and they may be small but they will exist.

A possible explanation for the failure of the H13 pin tool to support the setpoint normal force of 13,344 N is that the stress equivalent of 105 MPa exceeded the yield strength of the 6061/Al_2O_3 in the plasticized zone during this plunge test. If this occurred the 6061/Al_2O_3 would be incapable of supporting the setpoint load during the plunge with the H13 pin tool. This would require the temperature in the plasticized 6061/Al_2O_3 to exceed about 350°C [10]. In addition, the results in Fig. 1 suggest that higher temperatures were experienced in the 6061/Al_2O_3 using the H13 pin tool than those for either the WC10Co tool or the Si_3N_4 tool. Conditions under which this could occur will be discussed later.

The data plotted in Fig. 3 and Fig. 4 are referred to as effective friction coefficients because the measurement techniques and geometry do not lend themselves to an analysis that would yield a friction coefficient according to a classical treatment [11,12]. However, the normal force, and tool rotation speed of the plunge test do approximate those of actual friction stir welding. The flat face of the cylindrical pin tools also approximates the shape of friction stir welding tools without the complication of a pin or other intricate details of tool shape. Having test conditions that closely match application conditions is desirable when measuring friction properties [13]. Consequently, the effective friction coefficients given in Fig. 4 may then be considered representative of the actual friction conditons for those material couples during friction stir

welding. The effective friction coefficient values shown in Fig. 4 are also in the range of friction coefficients found for dry contact between other metal-metal couples [10,13], but somewhat higher than those between martensitic stainless steel and similar aluminum metal-matrix composites [14]. The increases of effective friction coefficient during the plunges were at least partially due to frictional drag between the pin shafts and plunge hole surfaces. This was evidenced by visible scuffing on the pin tool shaft surfaces after testing.

The variation of displacement rate with pin tool materials in the force-controlled segments of the plunge tests, shown in Fig. 5, was unexpected. As described earlier, the displacement rates in the force-controlled segments were not controlled by machine settings. Instead, the pin tools were free to plunge into the 6061/Al_2O_3 at rates determined by material properties and any interactions between the pin tool materials and the 6061/Al_2O_3. Because the pin tool materials were the only significant variable in the tests, they must have been responsible for the observed behavior.

One way of increasing displacement rate in this plunge test is by making the plate material easier to deform. How this could occur can be determined by considering the factors that contribute to frictional heating. Heat flow in friction stir welding has been treated using the Rosenthal approach [15] where it was shown that the temperature rise, ΔT, due to surface heating of a base material from a tool shoulder under constant pressure is:

$$\Delta T \propto \frac{\mu P \omega}{\lambda}$$

In this expression, μ is the friction coefficient, P is the pressure on the pin tool, ω is the rotation speed of the tool, and λ is the thermal conductivity of the base material. For the force controlled segments of the plunge tests all of these parameters are constant except for μ, which varied with pin tool material. Assuming that μ can be approximated by the μ_{eff} shown in Fig. 4, it can been seen that the temperature rises associated with the pin tools will rank with H13 as the highest, WC10Co as an intermediate value, and Si_3N_4 as the lowest. For a given increment of time, the H13 will heat the 6061/Al_2O_3 to a higher temperature than the other pin tool materials, and therefore should plunge into the plate at a higher rate as Fig. 5 shows. The effectiveness of heating for the H13-6061/Al_2O_3 couple undoubtedly contributed to the apparently anomalous behavior shown for normal force in Fig. 1.

Implicit in this analysis is the conclusion that plunge displacement rates as well as the temperature rises are proportional to μ_{eff}. However, the plunge displacement rate for the H13 pin tool was about 5 times higher than that of the Si_3N_4 tool, but its μ_{eff} was only about 1.6 times higher than that of the Si_3N_4. In addition, the thermal conductivities of H13 and Si_3N_4 are similar so that the difference in their plunge rates cannot be attributed solely to the effects of heat flow into the pin tools. This situation indicates that factors other than strictly frictional heating, such as viscous dissipation of mechanical energy in the plasticized zone of the 6061/Al_2O_3, contributed to the heating process.

From a practical point of view, the plunge displacement rate can be expected to also scale with maximum welding speed. Of course, tool life could be a much more important consideration

than welding speed, especially for metal-matrix composites. Wear behavior could ultimately dominate tool selection criteria for alloys such as 6061/Al_2O_3, and the duration of a plunge test may be too short to evaluate this aspect of tool properties.

The accumulation of plate material on the face of the H13 pin, shown in Fig. 6, suggests that it has a greater tendency for chemical reaction with the 6061/Al_2O_3 than either the WC10Co or the Si_3N_4. Further analysis will be required to determine the nature of the fracture of the 6061/Al_2O_3 at the bottom of the plunge hole and of its chemical reaction with the H13. However, the strength of the bonding at the H13-6061/Al_2O_3 interface must be relatively high considering the strength of the 6061/Al_2O_3. It seems likely that the nature of the interface contributed to the heating process in some way.

Conclusion

Flat-faced, cylindrical pin tools of H13 steel, WC10Co, and Si_3N_4 were plunged into 19-mm-thick plates of 6061+20wt%Al_2O_3 to depths of about 10 mm. The pin tools were rotated at 800 rpm. The plunge tests consisted of two segments. An initial plunge to a depth of 1.5 mm was used to seat the pins into the plate surfaces, and it was conducted at a constant displacement rate machine setting. The test segment beyond 1.5 mm was conducted using a force-control setting of 13,344 N. The displacement rate in the test segment was not controlled by machine settings.

The test results indicated that behavior during the plunges depended on the tool material. The measured normal force and spindle torque values were used to calculate effective friction coefficients for the three pin tool materials on the 6061/Al_2O_3. These values were: μ_{eff} = 1.024 for the H13, μ_{eff} = 0.768 for the WC10Co, and μ_{eff} = 0.621 for the Si_3N_4. The plunge displacement rates during force-controlled operation increased with μ_{eff} , and this behavior was consistent with heat flow analysis. The 6061/Al_2O_3 adhered to the H13 pin after the plunge test suggesting that chemical reaction between the pin tool and the plate contributed to the observed behavior.

Acknowledgement

MTS Corporation graciously provided access to their friction stir equipment for performing these experiments. Jack Halpin, Bobbi Edwards, and John Miller of MTS Corporation assisted with the experimentation and operation of the stir equipment. Review of the manuscript and helpful discussions by Dr. Peter Blau and Dr. Zhili Feng are greatly appreciated.

This research was sponsored by the U.S. Department of Energy, Assistant Secretary for Energy Efficiency and Renewable Energy, Office of FreedomCAR and Vehicle Technologies, as part of the High Strength Weight Reduction Materials Program, under contract DE-AC05-00OR22725 with ORNL operated by UT-Battelle, LLC for the U.S. Department of Energy.

This manuscript has been authored by a contractor of the U.S. Government under contract DE-AC05-00OR22725. Accordingly, the U.S. Government retains a nonexclusive, royalty-free license to publish of reproduce the published form of this contribution, or allow others to do so, for U.S. Government purposes.

References

1. *Welding Handbook, Volume 2, Welding Processes*, American Welding Society, Miami, FL, 1991
2. W. M. Thomas, E. D. Nicholas, J. C. Needham, M. G. Murch, P. Temple-Smith, and C. J. Dawes, "Improvements relating to friction welding," European Patent Specification EP 0 615 480 B1
3. W. M. Thomas and R. E. Dolby, "Friction Stir Welding Developments," pp. 203-211, *6th International Trends in Welding Research Conference Proceedings*, ASM International, Metals Park, Ohio, 2003
4. S. Kallee, "Application of friction stir welding in the shipbuilding industry," presented at Lightweight Construction – Latest Developments, The Royal Institution of Naval Architects, London, February 24-25, 2000, TWI website, http:\\www.twi.co.uk
5. W. J. Arbegast and P. J. Hartley, "Friction Stir Weld Technology Development at Lockheed Martin Michoud Space System-An Overview, pp. 541-546, *Trends in Welding Research, Proceeding of the 5th International Conference*, ASM International, Metals Park, Ohio, 1999
6. D. J. Waldron, R. W. Roberts, C. J. Dawes, and P. J. Tubby, "Friction Stir Welding Characterization for Aerospace Structures, pp. 547-552, *Trends in Welding Research, Proceeding of the 5th International Conference*, ASM International, Metals Park, Ohio, 1999
7. G. Oertelt, S. S. Babu, S. A. David, and E. A. Kenik, "Effect of Thermal Cycling on Friction Stir Welds of 2195 Aluminum Alloy, *Welding Journal Research Supplement*, vol. 80, no. 3, pp. 71-s-79-s, 2001
8. C. J. Cheng, "Transient Temperature Distribution During Friction Welding of Two Dissimilar Materials in Tubular Form, *Welding Journal Research Supplement*, vol. 42, no. 5, pp. 233-s-240-s, 1963.
9. T. J. Lienert, W. L. Stellwag, and H. Shao, "Determination of Load, Torque, and Tool Temperatures During Friction Stir Welding of Aluminum Alloys," EWI Summary Report SR0019, December 2000
10. *Smithells Metals Reference Book, Seventh Edition*, edited by E. A. Brandes and G. B. Brook, Butterworth-Heinemann, Woburn, Massachusetts, 1992
11. F. B. Bowden and D. Tabor, *The Friction and Lubrication of Solids*, Clarendon Press, 1950
12. E. Rabinowicz, *Friction and Wear of Materials*, J. Wiley & Sons, New York, NY, 1965
13. *ASM Handbook, Volume 18: Friction, Lubrication, and Wear Technology*, P. J. Blau, Volume Chairman, ASM International, Metals Park, Ohio, 1999
14. S. V. Prasad and K. R. Mecklenburg, "Friction behavior of ceramic fiber-reinforced aluminum metal-matrix composites against a 440C steel counterface," *Wear*, vol. 162, pp.47-56, 1993.
15. J. C. McClure, W. Tang, L. E. Murr, X. Guo, Z. Feng, and J. E. Gould, "A Thermal Model of Friction Stir Welding, pp. 590-595, *Trends in Welding Research, Proceeding of the 5th International Conference*, ASM International, Metals Park, Ohio, 1999

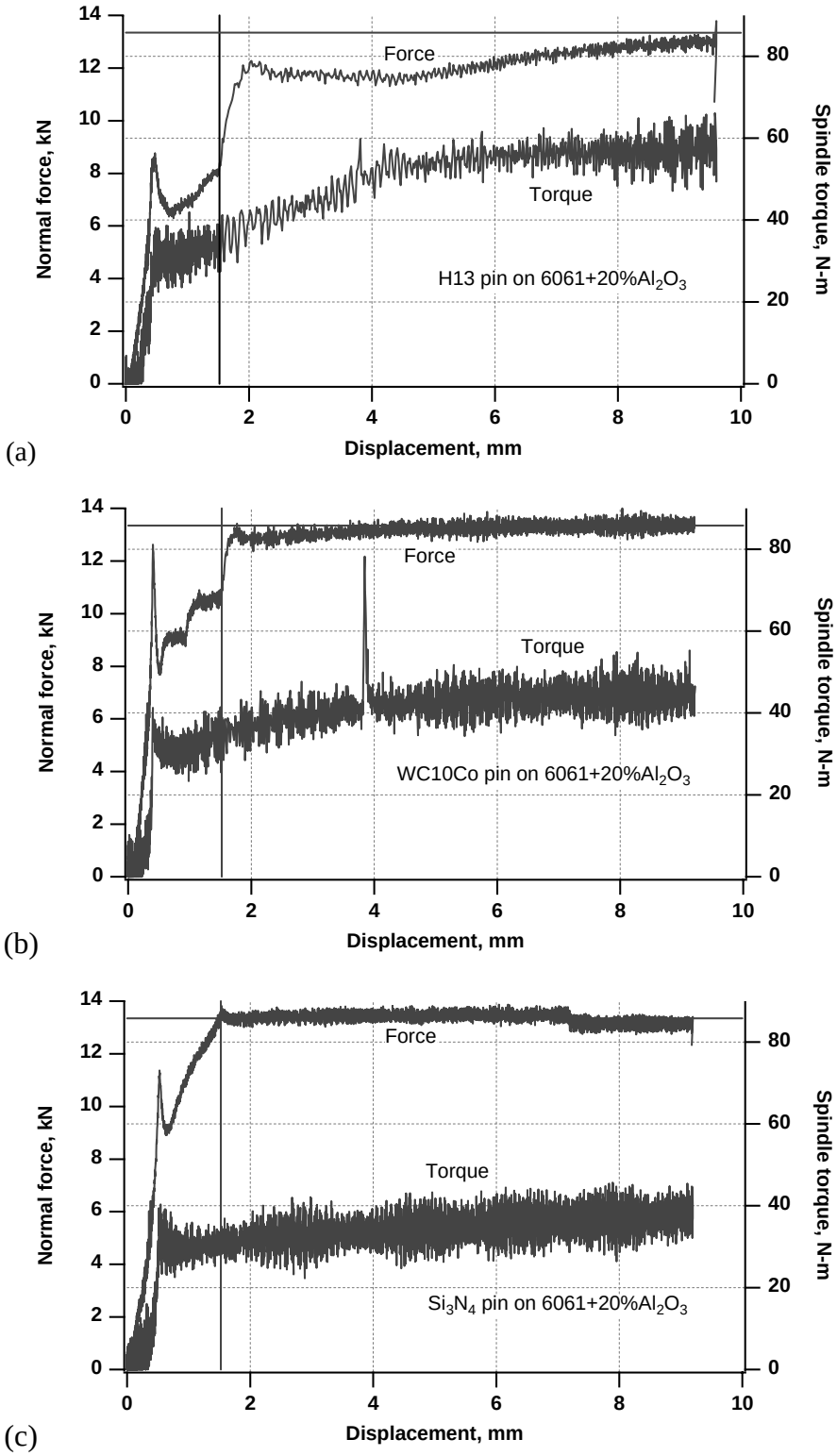

Fig. 1. Variations of normal force and spindle torque measured during plunging of pin tools of H13 steel (a), WC10Co (b), and Si_3N_4 (c), into 6061/Al_2O_3 plates.

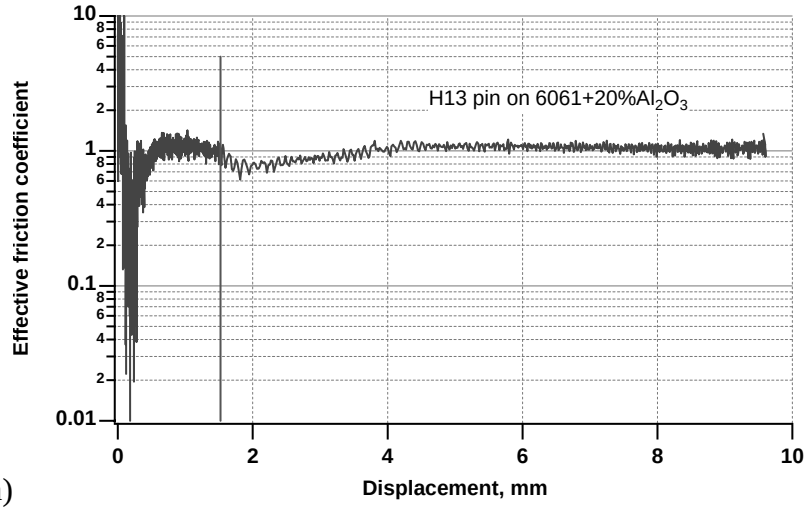

(a)

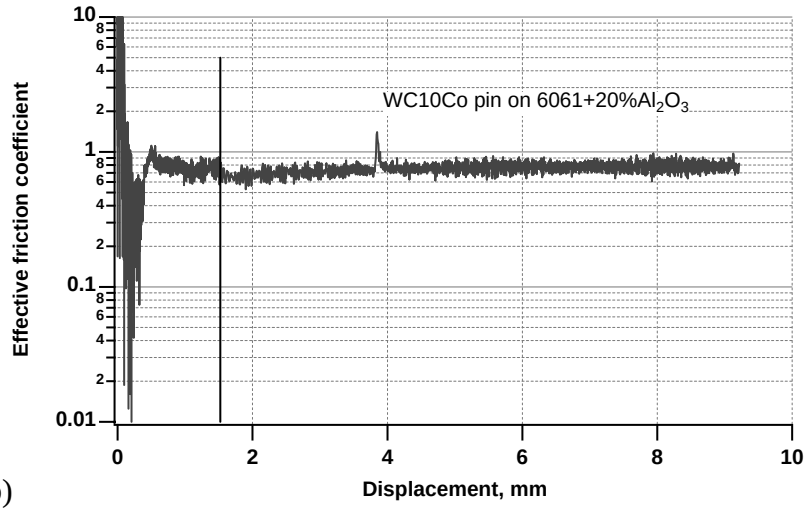

(b)

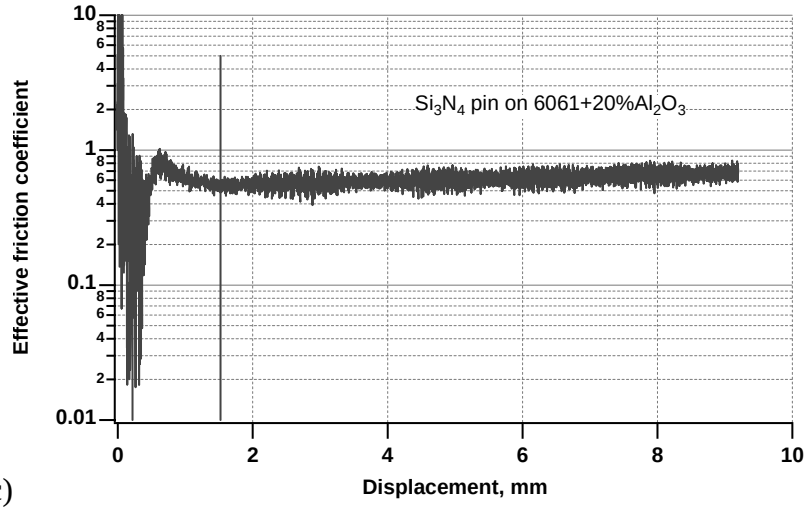

(c)

Fig. 3. Effective friction coefficients calculated from normal force and spindle torque measurements during plunging of pin tools of H13 steel (a), WC10Co (b), and Si_3N_4 (c), into 6061/Al_2O_3 plates.

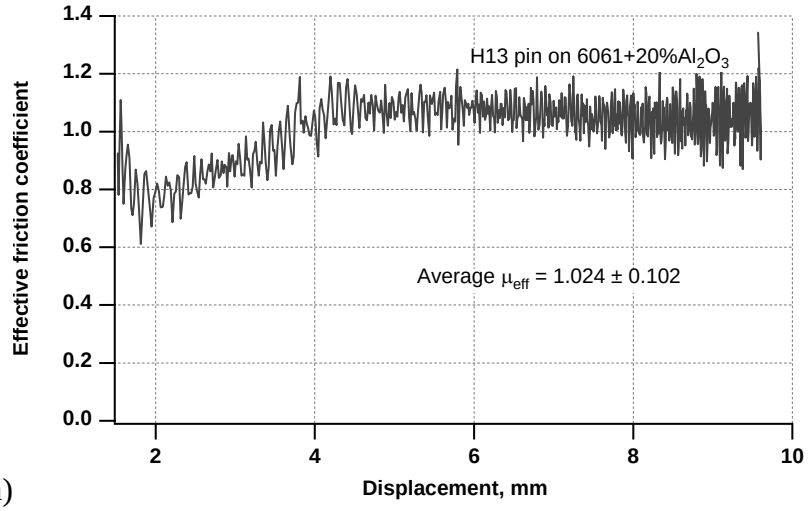

(a)

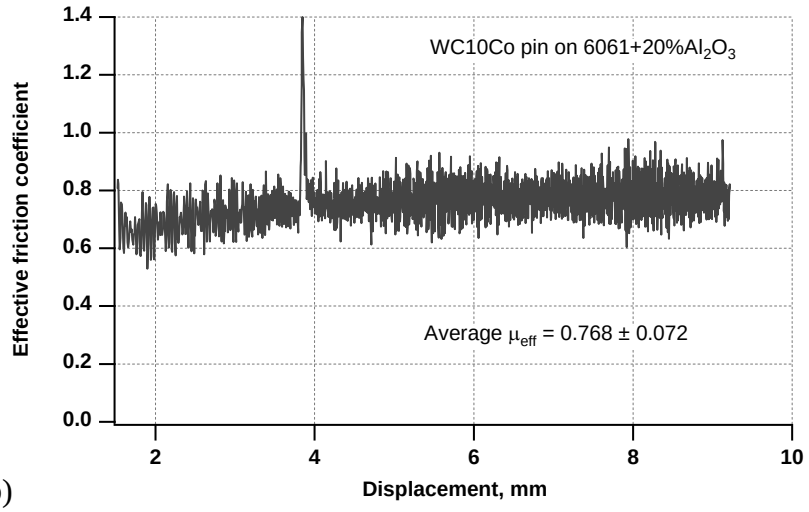

(b)

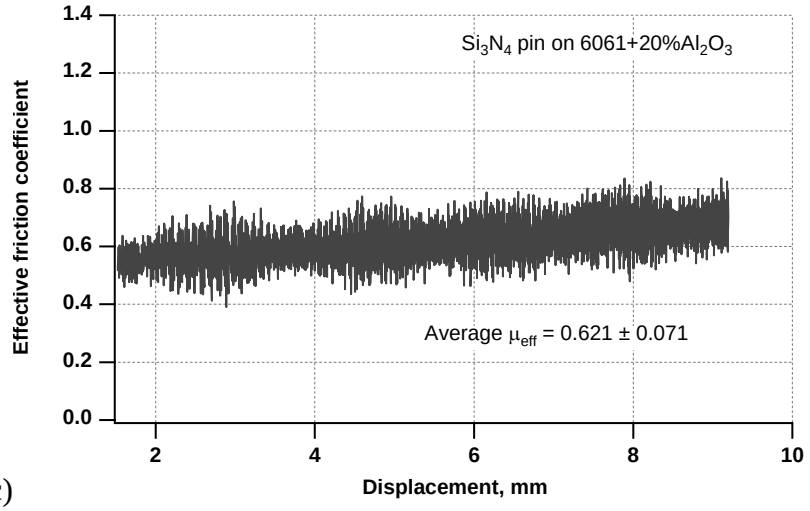

(c)

Fig. 4. Effective friction coefficients during force-controlled segments of plunging of pin tools of H13 steel (a), WC10Co (b), and Si_3N_4 (c), into 6061/Al_2O_3 plates.

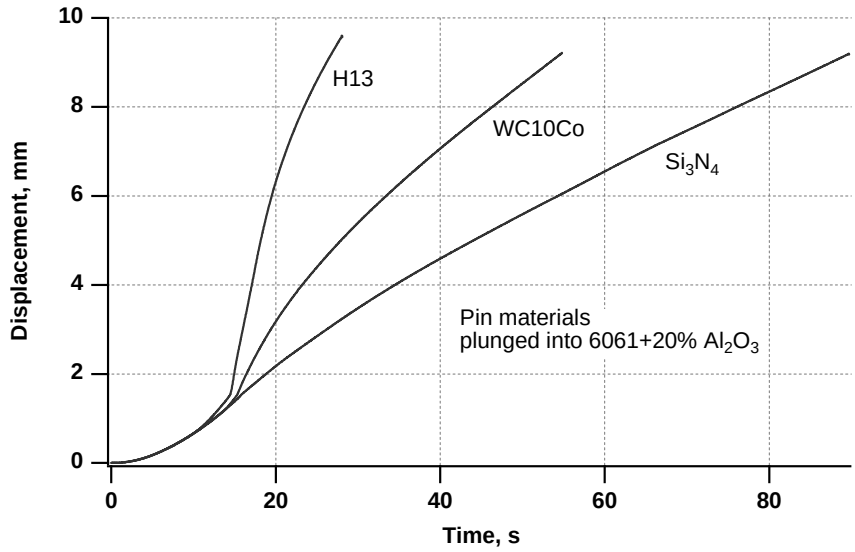

Fig. 5. Plunge displacement rates of H13, WC10Co, and Si_3N_4 pin tools into 6061/Al_2O_3 plate during force-controlled segments.

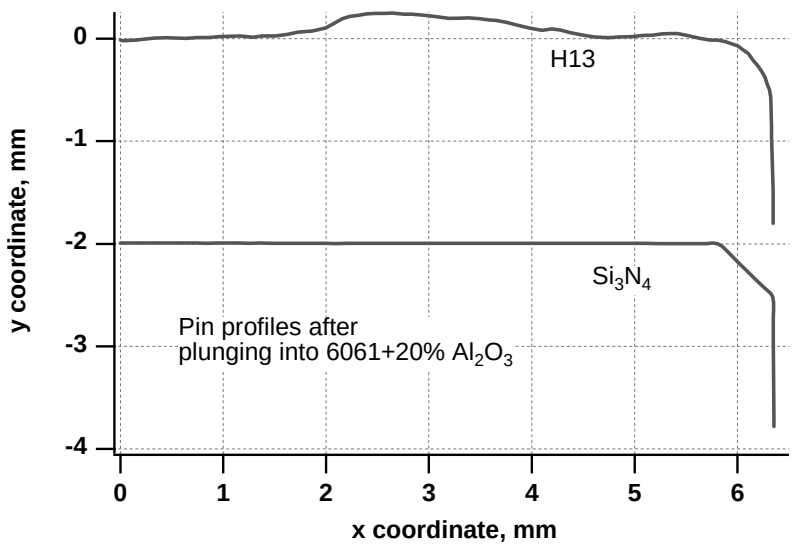

Fig. 6. Profiles of H13 and Si_3N_4 pin tools after plunging into 6061/Al_2O_3 plate.

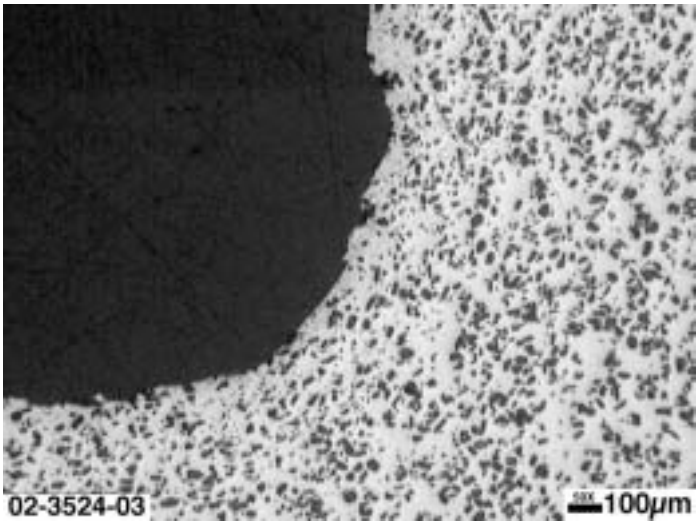

(a)

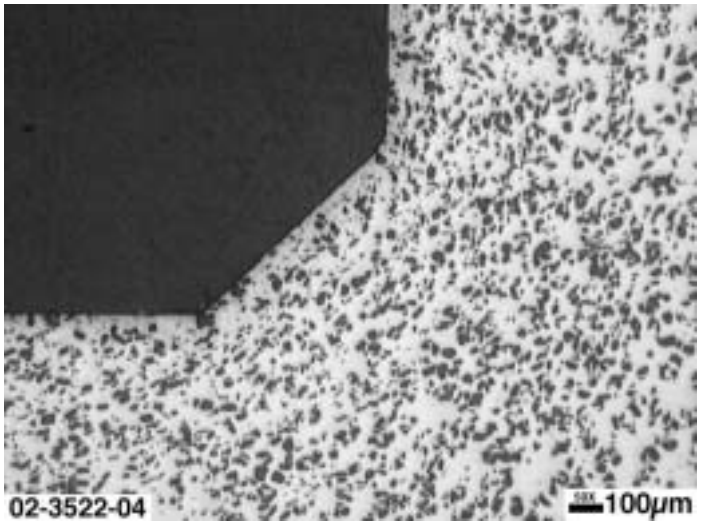

(b)

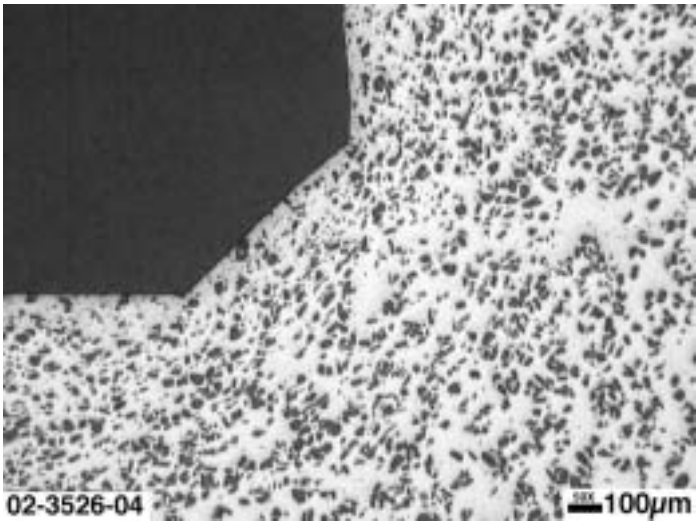

(c)

Fig. 7. Optical micrographs taken at the corners of the blind plunge holes made in 6061/Al_2O_3 plate with pin tools of (a) H13 steel, (b) WC10Co, and (c) Si_3N_4.